Transcriptomic Insights into Hypothalamic Aging During Menopause: A Comparative Analysis of Human and Mouse Models.

Authors: Jordana C. B. Bloom[1,2], Encarnacion Torres[2,3*], Sidney A. Pereira[2,3*], Liliana Arvizu-Sanchez[2], Audrey N. Fontes[2], Hadine Joffe[3,4,5], David C. Page[1,6,7], Victor M. Navarro[2,3,8]

Affiliations:

1. Whitehead Institute for Biomedical Research, Cambridge, MA 02142, USA
2. Division of Endocrinology, Diabetes and Hypertension, Brigham and Women's Hospital, Boston, MA 02115, USA
3. Harvard Medical School, Boston, MA 02115, USA
4. Division of Sleep Medicine, Brigham and Women's Hospital, Boston, MA 02115, USA
5. Mary Horrigan Connors Center for Women's Health and Gender Biology, Brigham and Women's Hospital, Boston MA 02115, USA
6. Department of Biology, Massachusetts Institute of Technology, Cambridge, MA 02139, USA
7. Howard Hughes Medical Institute, Cambridge, MA 02142, USA
8. Harvard Graduate Program in Neuroscience, Boston, MA 02115, USA

*Equal contribution.

Abstract

Menopause significantly impacts women's health, yet hypothalamic changes during this transition remain poorly understood. We analyzed gene expression in human hypothalamic samples across menopausal stages, revealing significant changes in inflammatory pathways, KNDy neuron signaling, and thermoregulatory genes. This analysis also identified novel central markers of menopause, including AKAP5 and CDKN1A (p21). To further investigate these changes, we developed a novel mouse model based on long-term (4 months) ovariectomy (OVX) that mimics the gonadotropin and temperature fluctuations of menopausal transition. Remarkably, the posterior hypothalamus of 4-month OVX mice closely mirrored the transcriptional changes observed in perimenopausal women. Both species exhibited increased inflammatory signaling and glial activation, alongside altered KNDy neuron activity. Our findings provide new insights into the central mechanisms of menopausal symptoms and offer a valuable preclinical model for testing interventions.

Introduction

Menopause marks a significant transition in women's lives, characterized by profound physiological changes that extend beyond reproductive function[1]. Understanding the neurobiological underpinnings of these changes is crucial for advancing women's health and developing targeted interventions for menopausal symptoms[2]. While much research has focused on ovarian function, our understanding of the central nervous system's role in menopausal transition, particularly the hypothalamus, remains limited[3].

The hypothalamus houses neuroendocrine centers that both control and are regulated by estrogens[4,5]. This bidirectional relationship positions the hypothalamus as a key player in the menopausal transition. As ovarian function declines and estrogen levels fluctuate, the hypothalamus undergoes significant adaptations, which in turn influence various physiological processes throughout the body[1,6-10]. Notably, these hypothalamic changes are implicated in the disruption of thermoregulation, sleep patterns, and the increased prevalence of mood disorders observed during menopause[7,10-16].

A subset of hypothalamic neurons known as KNDy neurons (named for their co-expression of kisspeptin, neurokinin B (NKB), and dynorphin A) have emerged as central players in the onset of vasomotor symptoms (VMS)[17]. VMS, which include hot flashes and night sweats, are among the most common and disruptive symptoms experienced by women during menopause[18]. The identification of KNDy neurons as triggers for VMS has opened new avenues for understanding and treating these symptoms[17,19]. These findings built on early works from Naomi Rance's group that described hypertrophy of NKB and substance P (SP) expressing neurons in the hypothalamus of post-menopausal women[4,20-23]. Despite these advances, our knowledge of the broader changes occurring in the hypothalamus during and after menopause, particularly regarding the onset, duration, and eventual resolution of menopausal symptoms, remains incomplete.

This gap in our understanding is further compounded by the limitations of current animal models of menopause[24]. While animal studies have provided valuable insights into some aspects of menopause, they often fail to fully recapitulate the complex changes observed in women during this transition. This limitation highlights a critical need for the development of new mouse models that more closely mimic the human menopausal experience, particularly with respect to hypothalamic changes.

The lack of comprehensive transcriptomic data from human hypothalamic tissue across different stages of menopause represents a significant barrier to progress in this field. Such data would not only enhance our understanding of the molecular mechanisms underlying menopausal symptoms, but also inform the development of more accurate animal models and potentially lead to novel therapeutic targets.

In this study, we address these knowledge gaps through a dual approach. First, we present a complete, unbiased transcriptomic analysis of hypothalamic samples from women across all menopausal stages. This unique analysis provides a detailed map of gene expression changes in the human hypothalamus throughout the menopausal transition, offering new insights into the molecular pathways involved in this process. Second, leveraging the insights gained from our human transcriptomic analysis, we have developed and characterized a new mouse model that closely resembles the changes observed in the human hypothalamus during menopause. This model represents a significant advancement in the field, providing a more accurate platform for studying menopausal processes and testing potential interventions.

By combining human and mouse transcriptomic data, our study aims to significantly enhance our understanding of the hypothalamic changes associated with menopause, while offering a preclinical platform to develop new approaches to manage menopausal symptoms.

Results

Identification and characterization of gene expression changes in the human hypothalamus across the menopausal transition

Utilizing publicly available RNA-sequencing data from the Genotype-Tissue Expression (GTEx) project[25], we investigated gene expression changes across the menopausal transition in the human hypothalamus. Female donors with hypothalamic tissue were included in our analyses if they passed GTEx donor eligibility criteria and their sequenced tissue had an RNA integrity number of 6 or greater (Supplementary Table 1). 31 samples from donors between the ages of 28 and 65 years old met our inclusion criteria (Fig. 1a) and samples were divided into five groups based upon menopause status[26,27], including pre-menopausal (< 45 years old), early peri-menopausal (46-50 years old), late peri-menopausal (51-55 years old), post-menopausal (56-60 years old) and late post-menopausal (61-65 years old) groups (Fig. 1b). Cell type deconvolution analyses of the bulk RNA-sequencing data revealed the presence of previously reported hypothalamic cell types[28] across all samples (Supplementary Fig. 1, Supplementary Table 2). To assess gene expression changes across the menopausal transition, we began by examining expression patterns across age in the cohort using locally estimated scatterplot smoothing (LOESS). Hierarchical clustering of LOESS expression profiles revealed distinct patterns across age, including genes with nearly constant (Fig. 1c), decreased (Fig. 1d), and increased (Fig. 1e) expression across age. Of particular interest was the identification of many genes with specific decreases (Fig. 1f) or increases (Fig. 1g) coinciding with menopausal transition timing (Supplementary Table 3).

The menopausal transition induces alterations in thermoregulatory signaling and hypothalamic inflammation

Next, we performed differential gene expression analyses[29] between the pre-menopausal group and the peri-menopausal and post-menopausal groups. Notably, gene set enrichment

130 analysis (GSEA)[30] revealed the highest and most significant enrichments in inflammatory pathway
131 signaling during late peri-menopause (Fig. 1h and Supplementary Table 4). Furthermore,
132 STRING analysis[31] of TNF-alpha hallmark pathway leading edge genes between late peri-
133 menopausal and pre-menopausal groups highlighted genes previously identified[32,33] to be
134 involved in thermoregulation, including fever responses (Fig. 1i).

135 Given the mounting scientific evidence implicating KNDy neurons in the onset of
136 vasomotor symptoms (VMS), we examined the expression of key ligand-receptor systems that
137 constitute the KNDy model, as well as critical regulatory genes, including *TAC1/TACR1* and
138 estrogen receptor α (*ESR1*). We plotted LOESS trajectories of these genes across age in the
139 human hypothalamus (Fig 2a). Our analysis revealed that while *KISS1R, TAC3, OPRK1*, and
140 *TACR1* did not display major changes throughout menopausal transition, they tended to increase
141 with age after menopause. However, *KISS1* and *ESR1* showed a marked increase throughout
142 menopause, as expected due to the decline in circulating estrogen, followed by a decline in
143 expression approximately 10 years after their menopausal peak. The expression of aromatase
144 (*CYP19A1*) showed a progressive increase with age but was unaffected by menopausal
145 transition. Interestingly, the changes in *KISS1* expression were inversely correlated with that of
146 the inhibitory dynorphin (*PDYN*) during this same transition, decreasing during menopause and
147 rising shortly after. *TACR3* expression, which is at the center of the mechanistic pathway that
148 triggers VMS, showed a marked increase in the years leading up to menopause, reaching
149 maximum expression at approximately 45 years of age. Thereafter, *TACR3* displayed a constant
150 decrease in expression, reaching minimal levels around 10 years post-menopause (Fig 2a).

151 We also examined the prostaglandin systems, which are involved in thermoregulation,
152 including fever[32,33]. Prostaglandin synthases 1 and 2 (*PTGS1/2*) increased their hypothalamic
153 expression with age during postmenopausal years. However, *PTGS2* also showed a marked
154 increase right at the beginning of menopausal transition (~50 years of age). Prostaglandin E
155 receptor 3 (*PTGER3*) increased right after menopause, followed by a sharp decrease around age

156 60 (Fig 2a). We also observed an increase with age in the expression of translocator protein
157 (*TSPO*), a marker of activated microglia, in late post-menopausal years, as previously reported[34].
158 Additionally, we noted an increase in the astrocyte activation markers *GFAP* and *VIM* during early
159 post-menopause. These trajectories in pro-inflammatory markers align with the pathways
160 identified in our GSEA (Fig 1h, i).
161
162 Based on our identification of thermoregulatory and inflammatory pathway changes during
163 the menopausal transition period, we performed an unbiased approach to identify genes of
164 interest. We conducted differential gene expression analysis between the late peri-menopausal
165 and pre-menopausal groups (Fig. 2b, Supplementary Table 5). We examined expression of the
166 identified differentially expressed genes across the defined age groups (Fig. 2c, Supplementary
167 Table 6) and plotted LOESS trajectories across age for the two identified genes with the most
168 statistically significant adjusted p-values, *AKAP5* and *CDKN1A* (Fig. 2d, e). We also assessed
169 expression of canonical aging-associated genes[35] across our groups (Supplementary Fig. 2a) and
170 plotted trajectories for genes with previously reported functions in brain aging and cognitive
171 decline[36-40] (Supplementary Fig. 2b). Many of the trajectories exhibited notable inflection points
172 during the late peri-menopausal years.
173
174 **Characterization of a novel mouse model of reproductive aging**
175 To experimentally model reproductive aging, we assessed a series of time points post-
176 OVX in mice (Fig. 3a). Serum luteinizing hormone (LH) concentrations increased progressively
177 compared to the intact model, with levels peaking at 2 months post-OVX before declining at 4
178 months post-OVX (Fig. 3b). Importantly, this observation mirrors what is observed over the course
179 of reproductive aging in women[26]. To characterize changes in thermoregulation, core temperature
180 was measured across time points in the model with a peak in core temperature observed at 14
181 days post-OVX (Fig. 3c). The increase in LH and temperature observed at 14 days post-OVX

182 resembles the changes observed in peri- and early menopause in women, while the decline in LH
183 and normalization of core temperature seen at 4 months post-OVX resemble the changes
184 observed in late post-menopausal women.

185 To further characterize this mouse model and determine whether these physiological
186 correlations between the rodent and the human extend to hypothalamic transcriptomic changes,
187 we performed bulk RNA-sequencing of the intact, 14 days (short-term) post-OVX and 4 months
188 (long-term) post-OVX models. We selected two regions of the hypothalamus to sequence based
189 on the localization of neurons controlling temperature regulation (preoptic area, POA) and the
190 localization of neurons controlling the metabolic and reproductive centers (posterior
191 hypothalamus, PH). Cell type deconvolution analyses of the bulk RNA-sequencing data revealed
192 the presence of previously reported hypothalamic cell types[28] across all samples just as in the
193 human dataset (Supplementary Fig. 3).

194 We then conducted differential gene expression[29] analyses between intact, short-term and
195 long-term post-OVX models in both the PH and POA. Among the differentially expressed genes,
196 *Gm28040*, which shares overlapping CDS with *Kiss1*, shows the largest expression change,
197 which was increased at 14 days and 4 month OVX in the PH and decreased in both groups in the
198 POA, resembling the known regulation of *Kiss1* in both hypothalamic areas[41]. This suggests that
199 in the mouse, *Gm28040* encodes a kisspeptin isoform (Fig 3 e-h, Supplementary Table 7).

200 Global gene set enrichment analysis revealed the greatest enrichment in inflammatory
201 pathways similar to what we identified in the human hypothalamus (Fig. 3d, Supplementary Table
202 8). STRING analysis[31] of TNF-alpha hallmark pathway leading edge genes in the POA also
203 identified genes related to thermoregulation (Supplemental Fig. 4). Volcano plots highlight
204 differentially expressed genes between labeled conditions and regions (Fig. 3e-h and
205 Supplemental Fig. 5a and b), with heatmaps showing how the identified genes are expressed
206 across conditions in the PH (Fig. 3i) and POA (Fig. 3j) (Supplementary Table 9).

207 Next, we examined the expression of previously identified marker genes for reproduction,
208 thermoregulation, and inflammation (particularly related to astrocyte and microglia activity) in both
209 the PH (Fig. 4a) and the POA (Fig. 4b), as we performed previously in human transcriptomic
210 samples (Fig 2). The expression of inflammation and astrocytic markers from gonad intact to 4
211 months post-OVX showed similar increasing trends to that observed in the human hypothalamus
212 across menopausal transition, with significant increases in *Vim*, *Iba1*, and *Tspo* in the PH, and in
213 the prostaglandin pathway (*Ptgs2*) in the POA. The "KNDy" genes, involved in reproductive and
214 thermoregulatory (VMS) control, are highly regulated by sex steroids[42], and thus they showed the
215 expected increase in expression in the PH (where the arcuate nucleus is located) in proportion to
216 time after OVX. The specific markers of temperature regulation assessed in this initial analysis
217 did not show significant changes after OVX.
218
219 **Comparative analyses of human and mouse hypothalamic reproductive aging**
220 A large proportion of expressed genes are shared between the human and mouse
221 hypothalamus (~77%) (Supplementary Fig. 6). Comparison of the GSEA results from the two
222 species revealed statistically significant pathway enrichment correlations between the two
223 datasets (Fig. 5a), further suggesting the suitability of this mouse model to assess hypothalamic
224 changes during menopause. To assess whether this correlation can be observed at the single
225 gene level, we selected *TACR3*, which has a documented role in the onset and severity of VMS[43].
226 Co-expression analyses identified genes whose expression positively correlated with *TACR3* (in
227 human) or *Tacr3* (in mouse) LOESS trajectories. These correlations revealed statistically
228 significant overlap in the positively regulated genes with *TACR3* in the two species (Fig. 5b,
229 Supplementary Table 10). We then hypothesized that if the short and long term OVX mouse
230 model is a good model to study hypothalamic transcriptomic changes throughout menopause, the
231 differentially expressed genes identified in the human samples should show similar trends in our
232 mouse model and vice versa. We depicted gene expression across the groups as heatmaps,

233 which show differentially expressed genes from the human dataset across mouse conditions (Fig.
234 5c, d) and mouse PH and POA datasets across human age groups (Fig. 5e, f). Remarkably, 2/3
235 of the differentially expressed genes identified in the human between 51-55 years showed a clear
236 increase at 4 months post-OVX, while the remaining 1/3 were captured at 14d post OVX in both
237 PH and POA. The opposite analysis revealed a majority of the genes that presented the highest
238 changes at 4 months post-OVX were upregulated in the 51-55 year old, late peri-menopausal,
239 group.

240 In sum, these findings indicate that the short-term and long-term post-OVX mouse models
241 described can be used as an experimental system to model hypothalamic changes in menopausal
242 women with a high degree of fidelity. Furthermore, our data reveal that while LH changes occur
243 relatively fast after OVX, the majority of hypothalamic transcriptomic changes that correlate with
244 perimenopause are not evident until 4 months post OVX (Fig 3), as also evidenced by pathway
245 correlation (Fig 5a). These data also reveal that the mouse PH resembles the whole human
246 hypothalamus better than the mouse POA.

247

248 **Neurokinin B distribution and neuroinflammatory markers in the reproductive aging**
249 **mouse models**

250 Further characterization of this mouse model was carried out at the protein level. To this
251 end, we continued our focus on the hypothalamic NKB/NK3R system. Unlike *Tac3* expression,
252 which increases with time after OVX (Fig 4), the expression of NKB decreased after OVX (Fig. 6).
253 This effect is expected for highly released neuropeptides, suggesting that this ligand is actively
254 being released rather than stored. To assess the activity of the arcuate nucleus (site of KNDy
255 neurons) after OVX, we stained for the early activation marker cFos. Importantly, this assay
256 revealed that cFos expression in the arcuate nucleus is significantly lower at 4 months compared
257 to 14 days post-OVX, and this was correlated with an increase in astrocytic activation, as shown
258 by Gfap staining, which correlates with the transcriptomic findings observed in human and mouse

259 transcriptomes. Nonetheless, these data could not answer whether the decrease in activity was
260 also at the level of the KNDy neuron or due to changes in other cells of the arcuate. Thus, we
261 quantified the changes in cFos within NKB neurons, which revealed a 50% decrease in activation.
262 Overall, we present a novel mouse model to study hypothalamic changes in menopausal
263 women and we used genes in the KNDy system to demonstrate the validity of this model.

264 **Discussion**

265 Our study utilizes transcriptomics from human hypothalamic samples across adult ages
266 to identify specific gene expression trends associated with aging and the menopausal transition
267 in women. Overall our findings offer new insights into the complex molecular landscape of the
268 aging hypothalamus and its response to declining ovarian function.

269 A key finding from our analysis is the increased inflammatory signaling in the
270 hypothalamus during late perimenopause, consistent with the concept of "inflammaging" that
271 develops with advanced age and contributes to various age-related pathologies[44]. Gene set
272 enrichment analysis revealed significant upregulation of inflammatory pathways, particularly TNF-
273 alpha signaling via NF-κB, during this transition period (Fig. 1h). Our STRING analysis of
274 differentially expressed genes highlighted several that are involved in thermoregulation and fever
275 responses (Fig. 1i), providing a potential mechanistic link between hypothalamic inflammation
276 and vasomotor symptoms commonly experienced during menopause. This neuroinflammatory
277 signature was further evidenced by increased expression of astrocyte activation markers *GFAP*
278 and VIM during early post-menopause, as well as the microglial marker *TSPO* in late
279 postmenopausal years (Fig. 2a). These findings align with previous studies showing astrocyte
280 and microglial reactivity in the aging brain[45]. Additionally, we observed age-associated increases
281 in prostaglandin synthesis enzymes *PTGS1/2*, which may contribute to neuroinflammation and
282 altered pain sensitivity in older women. Importantly, our mouse ovariectomy model recapitulated
283 these inflammatory changes, with gene set enrichment analysis showing significant enrichment
284 of inflammatory pathways at 4 months post-OVX (Fig. 3d), closely matching our findings in

285 perimenopausal women. We observed upregulation of glial activation markers and prostaglandin
286 synthesis enzymes in both the posterior hypothalamus (PH) and preoptic area (POA) (Fig. 4a,b),
287 mirroring the neuroinflammatory signature seen in aging human hypothalamus. This conserved
288 inflammatory response across species underscores its potential importance in driving age-related
289 changes in hypothalamic function.
290
291 We also assessed the changes in the expression of genes involved in reproductive
292 function and thermoregulation across the menopausal transition. As expected, *KISS1* expression
293 increased markedly during menopause[3,46], likely due to loss of estrogen negative feedback,
294 followed by a decline approximately 10 years post-menopause (Fig. 2a). This late-life reduction
295 in kisspeptin signaling may contribute to the eventual decline in gonadotropin levels seen years
296 after menopause onset[47,48]. Intriguingly, *TACR3* expression, which GWAS studies have
297 associated with the severity of VMS[43], showed a distinct pattern - increasing in the years leading
298 up to menopause, peaking around age 45, and then progressively declining (Fig. 2a). Given the
299 proposed role of neurokinin B signaling in triggering vasomotor symptoms[19,49], this expression
300 pattern aligns well with the typical time course of hot flashes, which often begin in perimenopause
301 and resolve within 5-10 years [50].
302
303 Unbiased differential expression analysis identified two genes, *AKAP5* and *CDKN1A*, as
304 particularly notable markers of the menopausal transition (Fig. 2b-e). *AKAP5* encodes a
305 scaffolding protein involved in synaptic plasticity[51-54] and showed increased expression in early
306 perimenopause. *CDKN1A*, encoding the cell cycle regulator p21,[55] was upregulated in late
307 perimenopause. Interestingly, p21 has been implicated in promoting senescence-associated
308 secretory phenotype (SASP)[55-58], in which senescent cells increase the secretion of inflammatory
309 factors, thus potentially contributing to the inflammatory phenotype we observed.
310

311 To determine whether these human transcriptomic changes could be modeled
312 experimentally, we developed a mouse ovariectomy (OVX) model with both short-term (14 day)
313 and long-term (4 month) timepoints. Remarkably, we found that the 4-month OVX timepoint
314 recapitulated many key features of human perimenopause. LH levels showed an initial increase
315 followed by decline (Fig. 3b), mirroring the human menopausal transition[26]. Core body
316 temperature was elevated at 14 days post-OVX but normalized by 4 months (Fig. 3c), paralleling
317 the typical time course of vasomotor symptoms[50]. Transcriptomic analysis of the mouse PH and
318 POA revealed striking similarities to the human dataset. Gene set enrichment analysis showed
319 significant enrichment of inflammatory pathways at 4 months post-OVX (Fig. 3d), closely matching
320 our findings in perimenopausal women. We observed upregulation of glial activation markers and
321 prostaglandin synthesis enzymes in both the PH and POA (Fig. 4a,b), recapitulating the
322 neuroinflammatory signature seen in aging human hypothalamus. Importantly, cross-species
323 comparison demonstrated significant correlation between the transcriptomic changes in our
324 human and mouse datasets (Fig. 5a). Nearly two-thirds of genes differentially expressed in late
325 peri-menopausal women showed concordant changes at 4 months post-OVX in mice, particularly
326 at the level of the PH where the early marker of menopause in humans *AKAP5* peaks 14d post
327 OVX and the maker of late peri-menopause, *CDKN1A*, showed the highest expression 4 months
328 post OVX (Fig 5c). This high degree of conservation suggests that our long term OVX model
329 effectively captures key molecular features of the human menopausal transition.
330
331 To further validate our model, we examined protein changes in neurokinin B (NKB)
332 expression and neuronal activation. Immunofluorescence staining revealed decreased NKB
333 levels in the arcuate nucleus at both 14 days and 4 months post-OVX (Fig. 6a-c,j). This contrasts
334 with the increased *Tac2* mRNA expression we observed and suggests enhanced NKB release
335 and depletion of peptide stores. Importantly, we found reduced c-Fos expression in NKB neurons
336 at 4 months post-OVX (Fig. 6m,n), indicating decreased neuronal activity. This aligns with the

337 declining *TACR3* expression seen in postmenopausal women and may reflect adaptive changes
338 to prolonged estrogen deficiency.
339
340 The age-related transcriptomic changes we identified likely have significant functional
341 consequences for hypothalamic physiology. Increased inflammatory signaling may disrupt the
342 precise neuroendocrine control of thermoregulation, metabolism, sleep, mood or cognition, all
343 critical symptoms of menopause. Astrocyte and microglial activation may impair normal neuronal
344 function through mechanisms that include altered glutamate uptake and synaptic pruning.
345
346 In conclusion, our findings offer significant potential for clinical applications. The
347 comprehensive transcriptomic data we've generated serves as a valuable resource for future
348 investigations into hypothalamic aging and the menopausal transition. Our validated mouse model
349 complements these findings by providing a platform for experimental manipulations, and
350 potentially allowing to determine the functional significance of specific molecular changes
351 observed in human samples. Together, these tools and insights pave the way for a deeper
352 understanding of menopause and the development of interventions that could significantly
353 improve women's health during this life stage.
354
355 **Methods**
356 **Mouse studies**
357 *Study approval and animals*
358 The animal studies were approved by the Brigham and Women's Hospital Institutional
359 Animal Care and Use Committee (IACUC) in the Center for Comparative Medicine. Adult wild-
360 type (WT) C57/BL6 female mice were group housed under constant conditions of temperature
361 (22–24°C) and light (12:12-hour light:dark cycle), fed with standard mouse chow and ad libitum
362 access to tap water.

363

364 *Experimental design*

365 To investigate the effects of sex steroids withdrawal on LH levels, core temperature (Tc),
366 and hypothalamic transcriptome profile, intact WT female mice were bilaterally ovariectomized
367 (OVX) to generate mouse models that would resemble pre-menopause, menopause transition
368 and early post-menopause in women. Blood LH levels and Tc were measured at baseline, when
369 females were still intact, at 7-, 14- and 21-days post OVX and at 1-, 2- and 4-months post OVX.
370 Additional females were euthanized before OVX in diestrus (pre-menopause group), after 14 days
371 of OVX (menopause transition group) or after 4 months of OVX (early post-menopause group)
372 and their posterior (PH) and preoptic area (POA) of the hypothalamus were collected for
373 transcriptome profile analysis by bulk RNA-seq.

374

375 *Ovariectomy (OVX)*

376 Adult (3-4 months-old) female mice were bilaterally OVX under isoflurane anesthesia.
377 Mice were treated with Buprenex SR (0.1 mg/kg, SC) and meloxicam (5 mg/kg, SC) on the day
378 of surgery. Mice were allowed to recover for at least 1 week before the start of experiments.

379 *Whole blood samples and LH Elisa*

380

381 For LH measurements, a 4μl blood sample was collected with a pipette. Whole blood was
382 immediately diluted in 116μl of 0.05% PBST [phosphate buffer saline (Boston Bio Products,
383 catalog #BM220) containing Tween-20 (Sigma, catalog #P2287)], vortexed, and frozen on dry ice.
384 Samples were stored at 80˚C until analyzed using an in-house sandwich enzyme-linked
385 immunosorbent assay as previously described Kreisman, et al. [59].

386

387 *Core temperature (Tc)*

388 For Tc measurements, intact female mice were implanted (intraperitoneally) with an IPTT-
389 300 temperature transponder (BioMedic Data Systems, Inc.). Tc from the transponder were
390 collected with a DAS-8007 Reader and DASHost 8000 software (BioMedic Data Systems, Inc.).
391
392 *Immunohistochemistry*
393 Animals were anesthetized with a ketamine/xylazine/saline cocktail and transcardially
394 perfused with saline (0.9% NaCl) followed by 4% paraformaldehyde (PFA) diluted in phosphate
395 buffer (PB) (Boston BioProducts, Inc). Brains were removed, stored in 4% PFA overnight and then
396 transferred into sucrose solution (30% sucrose in 0.1 M PB, Thermo Fisher Scientific) at 4˚C. After
397 sucrose infiltration, the tissue was frozen in Tissue-Tek® O.C.T. Compound (Sakura® Finetek-
398 4583) and cut on a freezing stage microtome (Microm HM 450, Thermo Fisher Scientific) into 30
399 µm coronal sections. Free-floating sections were washed in tris buffered saline (TBS, Boston
400 BioProducts, Inc) and blocked for 1 hour at room temperature in incubation solution [TBS +
401 0.3%Triton™ X-100 (Millipore Sigma) + 2% normal goat serum (NGS)]. Sections were
402 subsequently incubated for 48 hours at 4˚C with primary antibodies: rabbit-anti neurokinin B
403 (1:1000, Novus Biologicals, catalog #NB300-201), guinea pig anti-cFos (1:1000, Synaptic
404 System, catalog #226308) and mouse anti-GFAP (1:300, Cell Signaling, catalog #3670) diluted
405 in incubation solution. Next, sections were incubated for 1 hour at room temperature with
406 secondary antibodies: anti-rabbit Alexa Fluor 594 (1:500, Thermo Fisher Scientific, catalog
407 #A11012), anti-guinea pig Alexa Fluor 488 (1:500, Jackson ImmunoResearch, catalog
408 #706545148) and anti-mouse donkey Alexa 594 (1:500, Invitrogen, catalog #A32744). Sections
409 were mounted onto Super-frost plus glass slides (Fisher Laboratories), air dried and cover slipped
410 with Vectashield mounting medium with DAPI (Vector laboratories).
411
412 *Microscopy and image analysis*

413 The images were captured by using a fluorescent microscope (Leica DM 2500) in JPG
414 format and processed using the open-source software ImageJ, Fiji (National Institutes of Health,
415 Bethesda, Maryland). For image quantification, representative images of the areas of interest (i.e.,
416 ARC) were delimited using as reference the mouse section from Allen Brain Atlas [60]. Both sides
417 of bilateral ARC were counted on a similar number of sections and animal, and replicate values
418 were averaged.
419
420 *RNA extraction, library preparation, and sequencing*
421 Mouse posterior hypothalamus and preoptic area regions were dissected and flash frozen
422 prior to extracting RNA using a Zymo Quick RNA microprep kit according to the manufacturer's
423 instructions. RNA concentration was measured using a Qubit 4.0 fluorometer and the Quibit RNA
424 HS Assay Kit (ThermoFisher). All samples had RNA integrity numbers (RIN) greater than 7 as
425 measured on a Bioanalyzer 2100 instrument (Aligent). RNA sequencing libraries were prepared
426 using the KAPA mRNA HyperPrep–Stranded Kit (Roche) and sequenced on a NovaSeq SP
427 (Illumina) with 50bp paired-end reads.
428
429 *RNA-seq data processing and analysis*
430 We performed all analyses using mouse genome build mm39. To pseudoalign reads to
431 the transcriptome annotation and estimate expression levels of each transcript, we used kallisto[61]
432 in the tximport package[62] (v1.24.0). We imported the resulting count data (abundance.h5 file) into
433 R for analysis in DESeq2[29] (v1.36.0). To adjust for unknown, unmodeled or latent sources of
434 noise in the data we performed surrogate variable analysis (SVA) using the smartSVA package[63]
435 (v0.1.3) and used SV1 as a covariate in the differential gene expression analysis. Both
436 pseudoalignment and DESeq2 were performed on the entire transcriptome annotation, but, in
437 some cases, we restricted our downstream analysis to protein-coding genes, as annotated in

438 GENCODE version M30[64]. For gene set enrichment analysis (GSEA), we performed analyses
439 on pre-ranked ordered gene lists using the fgsea package[30] (v1.22.0).
440
441 *Prediction of protein interactions*
442 The first 30 leading edge genes from the comparison of the POA between female gonadal
443 intact vs. 4-month post-OVX mice were selected as the target gene list for TNF-α signaling
444 through NF-κB. The gene list was imported into STRING[65] for network reconstruction,
445 visualization and enrichment analysis [65]. Medium confidence, as the minimum required interaction
446 scored, was selected (0.400). Enrichment biological processed defined by gene ontology (GO)
447 were assessed. Of the top 10 variables identified by the GO terms, highlighted genes related to
448 thermoregulation and inflammation response to menopause transition are shown.
449
450 **Human studies**
451 *Human hypothalamus inclusion criteria*
452 Bulk RNA-sequencing read count data from human hypothalamus tissue was obtained
453 from publicly available Genotype-Tissue Expression (GTEx) Project[25] data. We included donor
454 tissue as part of our dataset if a sample met the following criteria: 1) donor eligibility criteria
455 (INCEXC) == TRUE, 2) tissue RNA quality score (RIN) >= 6, 3) donors were female (SEX == 2).
456
457 *Human data analysis*
458 After the sub-setting the GTEx RNA expression file for our samples of interest, we adjusted
459 for unknown, latent sources of noise in the data using SVA with the smartSVA package[63] (v0.1.3).
460 Differential expression analyses across age bins were performed using DESeq2[29] (v1.36.0) and
461 GSEA was performed on pre-ranked ordered gene lists using the fgsea package[30] (v1.22.0).
462 Gene expression trajectories across age (and parallel analyses across OVX conditions in mouse)

463 were performed on protein-coding genes using locally estimated scatterplot smoothing (LOESS)
464 similarly to Piehl et al. 2022[66]. Gene level output from LOESS across age was subjected to
465 expression trajectory correlation analysis. Genes were ranked based on their correlation with the
466 *TACR3/Tacr3* expression pattern. STRING interaction analyses were performed as described
467 above.
468
469 *Cell type decomposition analysis*
470 We performed cell type decomposition analyses to estimate the cell type composition of
471 our bulk RNA-seq datasets from human and mouse using the BisqueRNA package[67] (v1.0.5).
472 Table S5 lists the marker genes used to annotation cell types[28].
473
474 *Quantification and statistical analyses*
475 Various statistical tests were used to calculate p values as indicated in the methods
476 section, figure legends, or text, where appropriate. All statistics were calculated using R software,
477 version 4.2.1 unless stated otherwise. Results were considered statistically significant when $p <$
478 0.05 or FDR < 0.05 when multiple hypothesis correction was applied.
479
480 *Data and code availability*
481 - Raw RNA-seq data from mouse posterior hypothalamus and preoptic area regions have
482 been deposited to dbGAP and are publicly available as of the date of publication.
483 - This paper analyzes existing, publicly available GTEx consortium data available on the
484 GTEx Portal (https://www.gtexportal.org/home/).
485 - Original code to perform analyses will be publicly available as of the date of publication.
486 - Any additional information required to reanalyze the data reported in this study is available
487 from the lead contact upon request.

Acknowledgements: The Genotype-Tissue Expression (GTEx) Project was supported by the Common Fund of the Office of the Director of the National Institutes of Health (NIH), and by NCI, NHGRI, NHLBI, NIDA, NIMH, and NINDS. The data used for the analyses described in this manuscript were obtained from: the GTEx Portal on 08/10/22.

We also thank Whitehead Institute Genome Technology Core facility for library preparation and sequencing of mouse tissue samples.

Funding: This research was funded by NIH NICHD grants HD090151, HD099084, and NIA/ORWH grant U54 AG062322 to VMN and by The Brit Jepson d'Arbeloff Center on Women's Health to DCP.

Author contributions: J.C.B.B. performed all analyses of the human and mouse RNA-sequencing datasets. E.T.J. and S.A.P. performed all additional mouse experiments. J.C.B.B and V.M.N. wrote the manuscript. D.C.P., E.T.J. and S.A.P. revised the manuscript. D.C.P. and V.M.N. supervised all aspects of the work.

References

1 Davis, S. R. *et al.* Menopause. *Nature Reviews Disease Primers* **1**, 15004 (2015). https://doi.org/10.1038/nrdp.2015.4

2 Brinton, R. D., Yao, J., Yin, F., Mack, W. J. & Cadenas, E. Perimenopause as a neurological transition state. *Nature reviews. Endocrinology* **11**, 393-405 (2015). https://doi.org/10.1038/nrendo.2015.82

3 Rance, N. E. Menopause and the human hypothalamus: evidence for the role of kisspeptin/neurokinin B neurons in the regulation of estrogen negative feedback. *Peptides* **30**, 111-122 (2009). https://doi.org/10.1016/j.peptides.2008.05.016

4 Rance, N. E. & Uswandi, S. V. Gonadotropin-releasing hormone gene expression is increased in the medial basal hypothalamus of postmenopausal women. *J Clin Endocrinol Metab* **81**, 3540-3546 (1996). https://doi.org/10.1210/jcem.81.10.8855798

5 Herbison, A. E. in *Physiology of Reproduction* (ed J. Neil and E. Knobil) 1415–1482 (Academic Press, 2006).

6 Morselli, E. *et al.* The effects of oestrogens and their receptors on cardiometabolic health. *Nature reviews. Endocrinology* **13**, 352-364 (2017). https://doi.org/10.1038/nrendo.2017.12

7 Cohn, A. Y. *et al.* Effects of Sleep Fragmentation and Estradiol Decline on Cortisol in a Human Experimental Model of Menopause. *J Clin Endocrinol Metab* **108**, e1347-e1357 (2023). https://doi.org/10.1210/clinem/dgad285

8 Deecher, D. C. & Dorries, K. Understanding the pathophysiology of vasomotor symptoms (hot flushes and night sweats) that occur in perimenopause, menopause, and postmenopause life stages. *Arch Womens Ment Health* **10**, 247-257 (2007). https://doi.org/10.1007/s00737-007-0209-5

9 Maki, P. M. & Thurston, R. C. Menopause and Brain Health: Hormonal Changes Are Only Part of the Story. *Front Neurol* **11**, 562275 (2020). https://doi.org/10.3389/fneur.2020.562275

10 Reed, S. D., Newton, K. M., LaCroix, A. Z., Grothaus, L. C. & Ehrlich, K. Night sweats, sleep disturbance, and depression associated with diminished libido in late menopausal transition and early postmenopause: baseline data from the Herbal Alternatives for Menopause Trial (HALT). *Am J Obstet Gynecol* **196**, 593 e591-597; discussion 593 e597 (2007). https://doi.org/10.1016/j.ajog.2007.03.008

11 Ameratunga, D., Goldin, J. & Hickey, M. Sleep disturbance in menopause. *Intern Med J* **42**, 742-747 (2012). https://doi.org/10.1111/j.1445-5994.2012.02723.x

12 Augoulea, A. *et al.* Psychosomatic and vasomotor symptom changes during transition to menopause. *Prz Menopauzalny* **18**, 110-115 (2019). https://doi.org/10.5114/pm.2019.86835

13 Coborn, J. *et al.* Disruption of Sleep Continuity During the Perimenopause: Associations with Female Reproductive Hormone Profiles. *J Clin Endocrinol Metab* **107**, e4144-e4153 (2022). https://doi.org/10.1210/clinem/dgac447

14 Greendale, G. A., Karlamangla, A. S. & Maki, P. M. The Menopause Transition and Cognition. *JAMA* **323**, 1495-1496 (2020). https://doi.org/10.1001/jama.2020.1757

15 Kravitz, H. M. & Joffe, H. Sleep during the perimenopause: a SWAN story. *Obstet Gynecol Clin North Am* **38**, 567-586 (2011). https://doi.org/10.1016/j.ogc.2011.06.002

16 Landis, C. A. & Moe, K. E. Sleep and menopause. *Nurs Clin North Am* **39**, 97-115 (2004). https://doi.org/10.1016/j.cnur.2003.11.006

17 Koysombat, K., McGown, P., Nyunt, S., Abbara, A. & Dhillo, W. S. New advances in menopause symptom management. *Best Pract Res Clin Endocrinol Metab* **38**, 101774 (2024). https://doi.org/10.1016/j.beem.2023.101774

18 Freeman, E. W., Sammel, M. D., Lin, H., Liu, Z. & Gracia, C. R. Duration of menopausal hot flushes and associated risk factors. *Obstet Gynecol* **117**, 1095-1104 (2011). https://doi.org/10.1097/AOG.0b013e318214f0de

19 Prague, J. K. *et al.* Neurokinin 3 receptor antagonism as a novel treatment for menopausal hot flushes: a phase 2, randomised, double-blind, placebo-controlled trial. *Lancet* **389**, 1809-1820 (2017). https://doi.org/10.1016/s0140-6736(17)30823-1

20 Rance, N. E., McMullen, N. T., Smialek, J. E., Price, D. L. & Young, W. S., 3rd. Postmenopausal hypertrophy of neurons expressing the estrogen receptor gene in the human hypothalamus. *J Clin Endocrinol Metab* **71**, 79-85 (1990). https://doi.org/10.1210/jcem-71-1-79

21 Rance, N. E. & Young, W. S., 3rd. Hypertrophy and increased gene expression of neurons containing neurokinin-B and substance-P messenger ribonucleic acids in the hypothalami of postmenopausal women. *Endocrinology* **128**, 2239-2247 (1991).

22 Rance, N. E. Hormonal influences on morphology and neuropeptide gene expression in the infundibular nucleus of postmenopausal women. *Prog Brain Res* **93**, 221-235; discussion 235-226 (1992).

23 Chawla, M. K., Gutierrez, G. M., Young, W. S., 3rd, McMullen, N. T. & Rance, N. E. Localization of neurons expressing substance P and neurokinin B gene transcripts in the human hypothalamus and basal forebrain. *The Journal of comparative neurology* **384**, 429-442 (1997).

24 Koebele, S. V. & Bimonte-Nelson, H. A. Modeling menopause: The utility of rodents in translational behavioral endocrinology research. *Maturitas* **87**, 5-17 (2016). https://doi.org/10.1016/j.maturitas.2016.01.015

25 Lonsdale, J. *et al.* The Genotype-Tissue Expression (GTEx) project. *Nature Genetics 2013 45:6* **45** (2013-05-29). https://doi.org/10.1038/ng.2653

26 Soares, A. G. *et al.* Longitudinal changes in reproductive hormones through the menopause transition in the Avon Longitudinal Study of Parents and Children (ALSPAC). *Scientific Reports 2020 10:1* **10** (2020-12-04). https://doi.org/10.1038/s41598-020-77871-9

27 Khoudary, S. R. E. *et al.* The menopause transition and women's health at midlife: a progress report from the Study of Women's Health Across the Nation (SWAN). *Menopause (New York, N.y.)* **26** (2019/10). https://doi.org/10.1097/GME.0000000000001424

28 Hajdarovic, K. H. *et al.* Single-cell analysis of the aging female mouse hypothalamus. *Nature Aging 2022 2:7* **2** (2022-07-04). https://doi.org/10.1038/s43587-022-00246-4

29 Love, M. I. *et al.* Moderated estimation of fold change and dispersion for RNA-seq data with DESeq2. *Genome Biology 2014 15:12* **15** (2014-12-05). https://doi.org/10.1186/s13059-014-0550-8

30 Korotkevich, G. *et al.* Fast gene set enrichment analysis. *BioRxiv* (2021-02-01). https://doi.org/10.1101/060012

31 The STRING database in 2021: customizable protein-protein networks, and functional characterization of user-uploaded gene/measurement sets - PubMed. *Nucleic Acids Res* **49** (01/08/2021). https://doi.org/10.1093/nar/gkaa1074

32 Blomqvist, A. & Engblom, D. Neural Mechanisms of Inflammation-Induced Fever. *The Neuroscientist* **24** (2018/08). https://doi.org/10.1177/1073858418760481

33 Prostaglandin production selectively in brain endothelial cells is both necessary and sufficient for eliciting fever - PubMed. *Proc Natl Acad Sci USA* **119** (10/25/2022). https://doi.org/10.1073/pnas.2122562119

34 Butler, T. *et al.* Positron Emission Tomography reveals age-associated hypothalamic microglial activation in women. *Sci Rep* **12**, 13351 (2022). https://doi.org/10.1038/s41598-022-17315-8

35 Tacutu, R. *et al.* Human Ageing Genomic Resources: new and updated databases. *Nucleic Acids Res* **46** (2018/01/01). https://doi.org/10.1093/nar/gkx1042

36 O'Day, D. H. Calmodulin Binding Proteins and Alzheimer's Disease: Biomarkers, Regulatory Enzymes and Receptors That Are Regulated by Calmodulin. *Int J Mol Sci* **21** (2020/10). https://doi.org/10.3390/ijms21197344

37 Kim, J., Basak, J. M. & Holtzman, D. M. The Role of Apolipoprotein E in Alzheimer's Disease. *Neuron* **63** (2009/08/13). https://doi.org/10.1016/j.neuron.2009.06.026

38 Bateman, R. J. *et al.* Clinical and Biomarker Changes in Dominantly Inherited Alzheimer's Disease. *New England Journal of Medicine* **367** (2012-08-30). https://doi.org/10.1056/NEJMoa1202753

39 SIRT1 in Neurodevelopment and Brain Senescence. *Neuron* **81** (2014/02/05). https://doi.org/10.1016/j.neuron.2014.01.028

40 Catechol-O-methyltransferase polymorphisms and some implications for cognitive therapeutics - PubMed. *NeuroRx : the journal of the American Society for Experimental NeuroTherapeutics* **3** (2006 Jan). https://doi.org/10.1016/j.nurx.2005.12.010

41 Smith, J. T., Cunningham, M. J., Rissman, E. F., Clifton, D. K. & Steiner, R. A. Regulation of Kiss1 gene expression in the brain of the female mouse. *Endocrinology* **146**, 3686-3692 (2005). https://doi.org/10.1210/en.2005-0488

42 Goodman, R. L., Herbison, A. E., Lehman, M. N. & Navarro, V. M. Neuroendocrine control of gonadotropin-releasing hormone: Pulsatile and surge modes of secretion. *Journal of neuroendocrinology* **34**, e13094 (2022). https://doi.org/10.1111/jne.13094

43 Crandall, C. J. *et al.* Association of genetic variation in the tachykinin receptor 3 locus with hot flashes and night sweats in the Women's Health Initiative Study. *Menopause* **24**, 252-261 (2017). https://doi.org/10.1097/gme.0000000000000763

44 Franceschi, C., Garagnani, P., Vitale, G., Capri, M. & Salvioli, S. Inflammaging and 'Garb-aging'. *Trends Endocrinol Metab* **28**, 199-212 (2017). https://doi.org/10.1016/j.tem.2016.09.005

45 Clarke, L. E. *et al.* Normal aging induces A1-like astrocyte reactivity. *Proceedings of the National Academy of Sciences of the United States of America* **115**, E1896-e1905 (2018). https://doi.org/10.1073/pnas.1800165115

46 Rometo, A. M., Krajewski, S. J., Voytko, M. L. & Rance, N. E. Hypertrophy and increased kisspeptin gene expression in the hypothalamic infundibular nucleus of postmenopausal women and ovariectomized monkeys. *J Clin Endocrinol Metab* **92**, 2744-2750 (2007). https://doi.org/10.1210/jc.2007-0553

47 Hall, J. E. Neuroendocrine physiology of the early and late menopause. *Endocrinology and Metabolism Clinics* **33** (2004/12/01). https://doi.org/10.1016/j.ecl.2004.08.002

48 Hall, J. E., Lavoie, H. B., Marsh, E. E. & Martin, K. A. Decrease in Gonadotropin-Releasing Hormone (GnRH) Pulse Frequency with Aging in Postmenopausal Women*. *The Journal of Clinical Endocrinology & Metabolism* **85** (2000/05/01). https://doi.org/10.1210/jcem.85.5.6612

49 Christ, J. P., Navarro, V. M. & Reed, S. D. Nonhormonal Therapies for Menopausal Vasomotor Symptoms. *Jama* **330**, 1278-1279 (2023). https://doi.org/10.1001/jama.2023.15965

50 Avis, N. E. *et al.* Duration of Menopausal Vasomotor Symptoms. *JAMA Internal Medicine* **175** (2015/04/01). https://doi.org/10.1001/jamainternmed.2014.8063

51 He, Z. *et al.* Novel insight into the role of A-kinase anchoring proteins (AKAPs) in ischemic stroke and therapeutic potentials. *Biomedicine & Pharmacotherapy* **175**, 116715 (2024). https://doi.org/https://doi.org/10.1016/j.biopha.2024.116715

52 Koster, K. P. *et al.* Akap5 links synaptic dysfunction to neuroinflammatory signaling in a mouse model of infantile neuronal ceroid lipofuscinosis. *Front Synaptic Neurosci* **16**, 1384625 (2024). https://doi.org/10.3389/fnsyn.2024.1384625

53 Sanderson, J. L. & Dell'Acqua, M. L. AKAP signaling complexes in regulation of excitatory synaptic plasticity. *Neuroscientist* **17**, 321-336 (2011). https://doi.org/10.1177/1073858410384740

54 Weisenhaus, M. *et al.* Mutations in AKAP5 disrupt dendritic signaling complexes and lead to electrophysiological and behavioral phenotypes in mice. *PloS one* **5**, e10325 (2010). https://doi.org/10.1371/journal.pone.0010325

55 Engeland, K. Cell cycle regulation: p53-p21-RB signaling. *Cell Death & Differentiation* **29**, 946-960 (2022). https://doi.org/10.1038/s41418-022-00988-z

56 Wagner, K. D. & Wagner, N. The Senescence Markers p16INK4A, p14ARF/p19ARF, and p21 in Organ Development and Homeostasis. *Cells* **11** (2022). https://doi.org/10.3390/cells11121966

57 Wang, L., Lankhorst, L. & Bernards, R. Exploiting senescence for the treatment of cancer. *Nature Reviews Cancer* **22**, 340-355 (2022). https://doi.org/10.1038/s41568-022-00450-9

58 Chinta, S. J. *et al.* Cellular senescence and the aging brain. *Exp Gerontol* **68**, 3-7 (2015). https://doi.org/10.1016/j.exger.2014.09.018

59 Kreisman, M. J., McCosh, R. B. & Breen, K. M. A Modified Ultra-Sensitive ELISA for Measurement of LH in Mice. *Endocrinology* **163** (2022/09). https://doi.org/10.1210/endocr/bqac109

60 Wang, Q. *et al.* The Allen Mouse Brain Common Coordinate Framework: A 3D Reference Atlas. *Cell* **181**, 936-953 e920 (2020). https://doi.org/10.1016/j.cell.2020.04.007

61 Bray, N. L. *et al.* Near-optimal probabilistic RNA-seq quantification. *Nature Biotechnology 2016 34:5* **34** (2016-04-04). https://doi.org/10.1038/nbt.3519

62 Soneson, C., Love, M. I. & Robinson, M. D. Differential analyses for RNA-seq: transcript-level estimates improve gene-level inferences - PubMed. *F1000Res* **4** (12/30/2015). https://doi.org/10.12688/f1000research.7563.2

63 Chen, J. *et al.* Fast and robust adjustment of cell mixtures in epigenome-wide association studies with SmartSVA - PubMed. *BMC genomics* **18** (05/26/2017). https://doi.org/10.1186/s12864-017-3808-1

64 Frankish, A. *et al.* GENCODE reference annotation for the human and mouse genomes. *Nucleic Acids Res* **47** (2019/01/01). https://doi.org/10.1093/nar/gky955

65 Szklarczyk, D. *et al.* STRING v11: protein-protein association networks with increased coverage, supporting functional discovery in genome-wide experimental datasets. *Nucleic Acids Res* **47**, D607-D613 (2019). https://doi.org/10.1093/nar/gky1131

66 Piehl, N. *et al.* Cerebrospinal fluid immune dysregulation during healthy brain aging and cognitive impairment. *Cell* **185** (2022/12/12). https://doi.org/10.1016/j.cell.2022.11.019

67 Jew, B. *et al.* Accurate estimation of cell composition in bulk expression through robust integration of single-cell information. *Nature Communications 2020 11:1* **11** (2020-04-24). https://doi.org/10.1038/s41467-020-15816-6

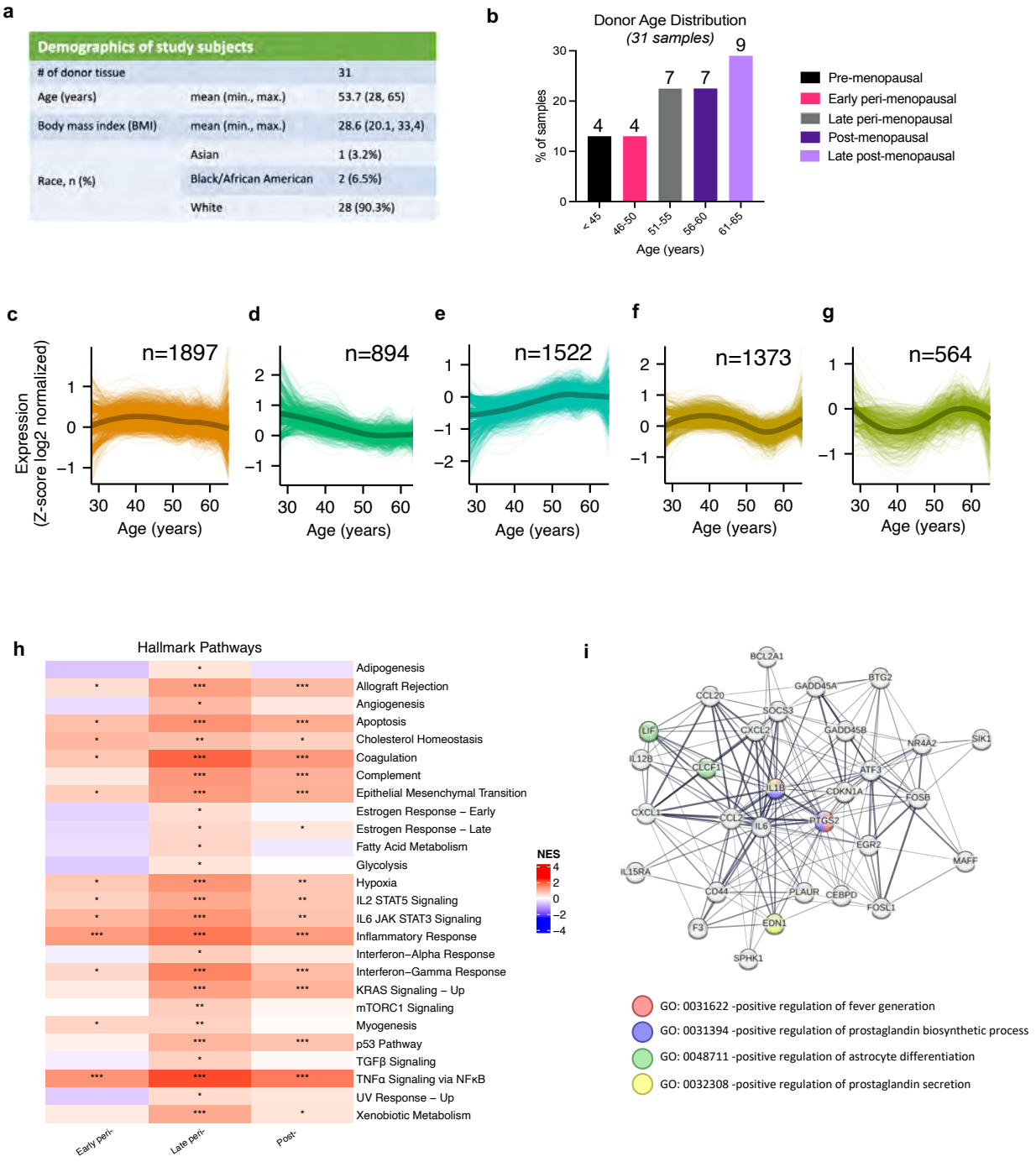

Figure 1. Gene expression changes across the menopausal transition in the human hypothalamus reveal alterations in thermoregulatory and inflammatory signaling.

a) Demographic overview of the GTEx donor subset used in this study.

b) Distribution of ages within the donor cohort and the defined age groupings for subsequent analyses.

c-g) Sets of genes grouped by hierarchical clustering and displayed using LOESS trajectories, **c)** constant expression across age, **d)** decreased expression across age, **e)** increased expression across age, **f)** decreased expression during the peri-menopausal transition, **g)** increased expression during the peri-menopausal transition.

h) Heatmap of normalized enrichment scores (NES) for Hallmark gene sets in which there was a statistically significant pathway enrichment in at least one of the three comparisons; significant enrichments indicated by asterisks (* p-adj <0.05; ** p-adj < 0.01; *** p-adj < 0.001)

i) STRING analysis of TNF-alpha hallmark pathway leading edge genes between the late peri-menopausal vs. pre-menopausal groups.

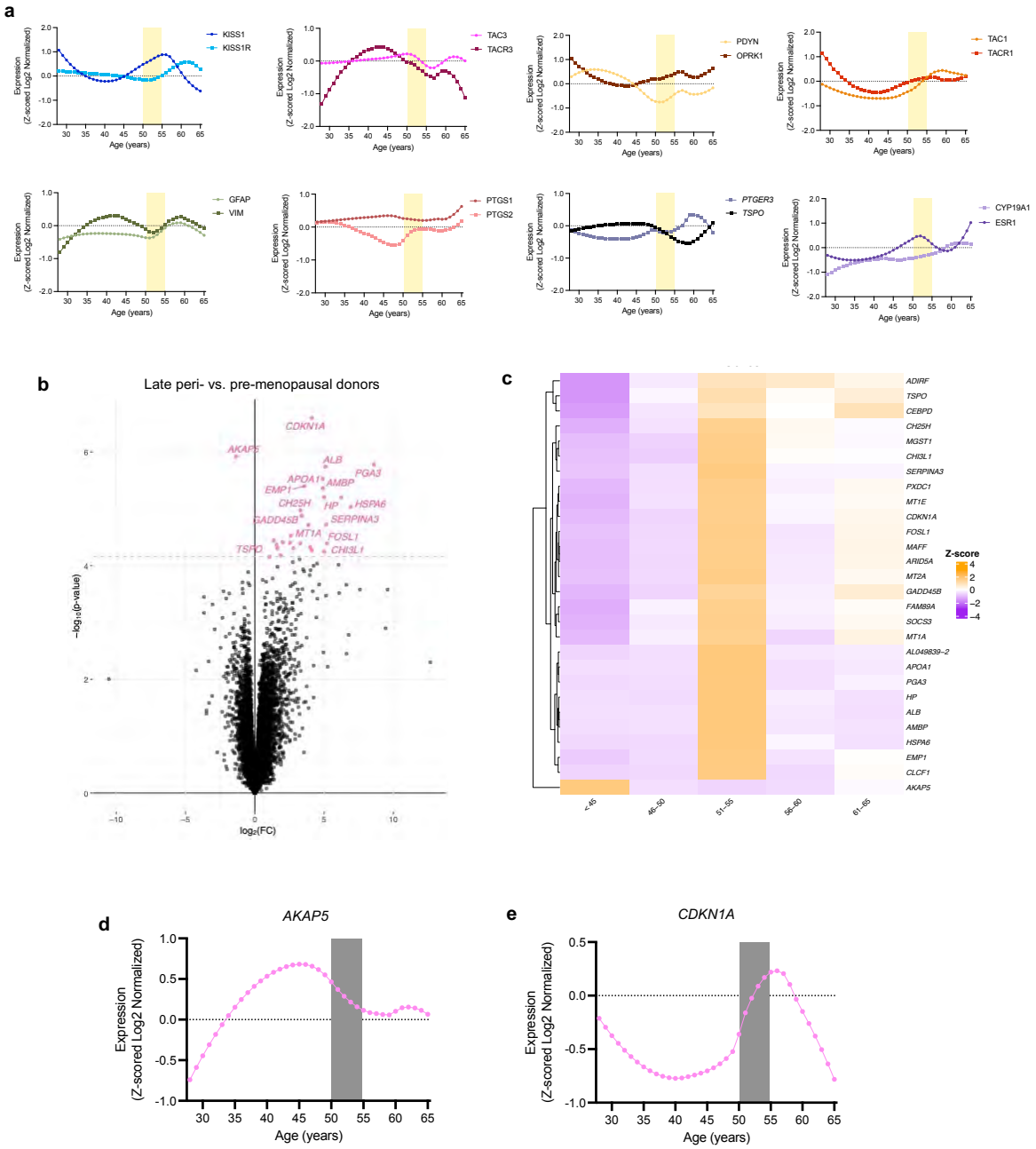

Figure 2. Expression of reproductive- and aging-related genes during the menopausal transition in the human hypothalamus.

a) Expression of KNDy genes and their receptors, thermoregulatory genes, astrocyte-, and microglia-marker genes across age in human hypothalamus tissue.
b) Volcano plot highlighting significantly differentially expressed genes between late peri- and pre-menopausal groups. Genes with a FDR < 0.05 are highlighted in pink.
c) Heatmap of genes identified in **b** and their expression across age groups.
d) Expression of *AKAP5* across age in human hypothalamus tissue.
e) Expression of *CDKN1A* across age in human hypothalamus tissue.

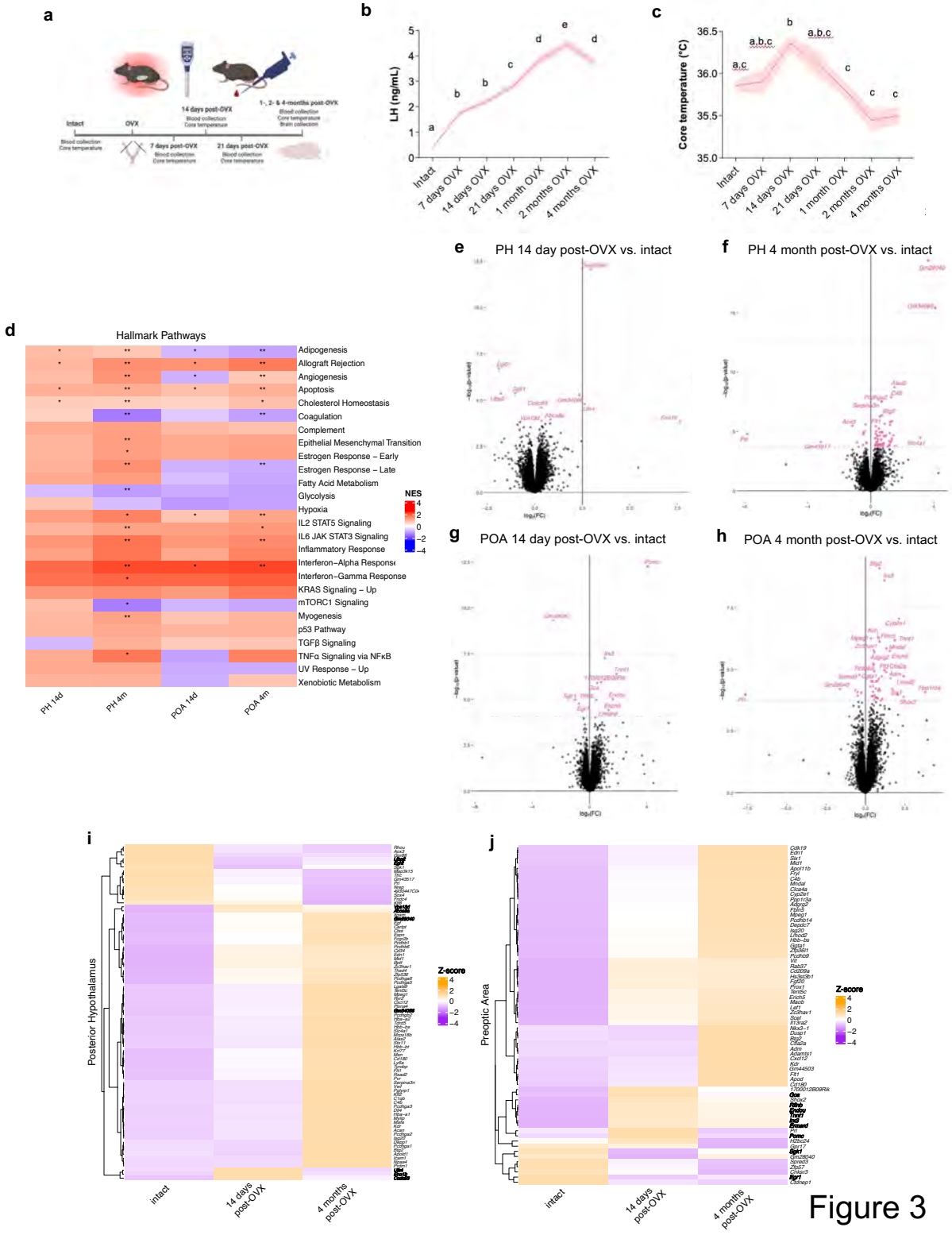
a
Intact
OVX
14 days post-OVX
1-, 2- & 4-months post-OVX
7 days post-OVX
21 days post-OVX
b
LH (ng/mL)
Intact
7 days OVX
14 days OVX
21 days OVX
1 month OVX
2 months OVX
4 months OVX
c
Core temperature (°C)
d
Hallmark Pathways
Adipogenesis
Allograft Rejection
Angiogenesis
Apoptosis
Cholesterol Homeostasis
Coagulation
Complement
Epithelial Mesenchymal Transition
Estrogen Response – Early
Estrogen Response – Late
Fatty Acid Metabolism
Glycolysis
Hypoxia
IL2 STAT5 Signaling
IL6 JAK STAT3 Signaling
Inflammatory Response
Interferon–Alpha Response
Interferon–Gamma Response
KRAS Signaling – Up
mTORC1 Signaling
Myogenesis
p53 Pathway
TGFβ Signaling
TNFα Signaling via NFκB
UV Response – Up
Xenobiotic Metabolism
NES
PH 14d
PH 4m
POA 14d
POA 4m
e PH 14 day post-OVX vs. intact
f PH 4 month post-OVX vs. intact
g POA 14 day post-OVX vs. intact
h POA 4 month post-OVX vs. intact
i
Posterior Hypothalamus
Z-score
intact
14 days post-OVX
4 months post-OVX
j
Preoptic Area
Z-score
intact
14 days post-OVX
4 months post-OVX

Figure 3

Figure 3. Physiological and transcriptomic changes in post-ovariectomy mouse models recapitulate key features of reproductive aging.

a) Schematic representation of the experimental design.
b) Luteinizing Hormone (LH) concentration in serum isolated from whole blood 7-, 14-, 21-days post-OVX and 1-, 2- and 4-months post-OVX in wild-type female mice (n=20, per condition).
c) Core temperature (ºC) measurements at 7-, 14-, 21-days post-OVX and 1-, 2- and 4-months post-OVX in wild-type female mice (n=20, per condition). b-c) Data values are shown as mean ± SEM. Groups with different letters are significantly from each other, $P < 0.05$ by One-way ANOVA/Tukey.
d) Heatmap of normalized enrichment scores (NES) for Hallmark gene sets in the Posterior Hypothalamus (PH) and the Preoptic Area (POA); significant enrichments indicated by asterisks (* *p*-adj <0.05; ** *p*-adj < 0.01; *** *p*-adj < 0.001)

e-h) Volcano plots highlighting significantly differentially expressed genes between labeled conditions and regions. Genes with a FDR < 0.05 are labeled in pink.

i) Heatmap of PH DE genes identified in **b** and their expression across conditions.

j) Heatmap of POA DE genes identified in **d** and their expression across conditions.

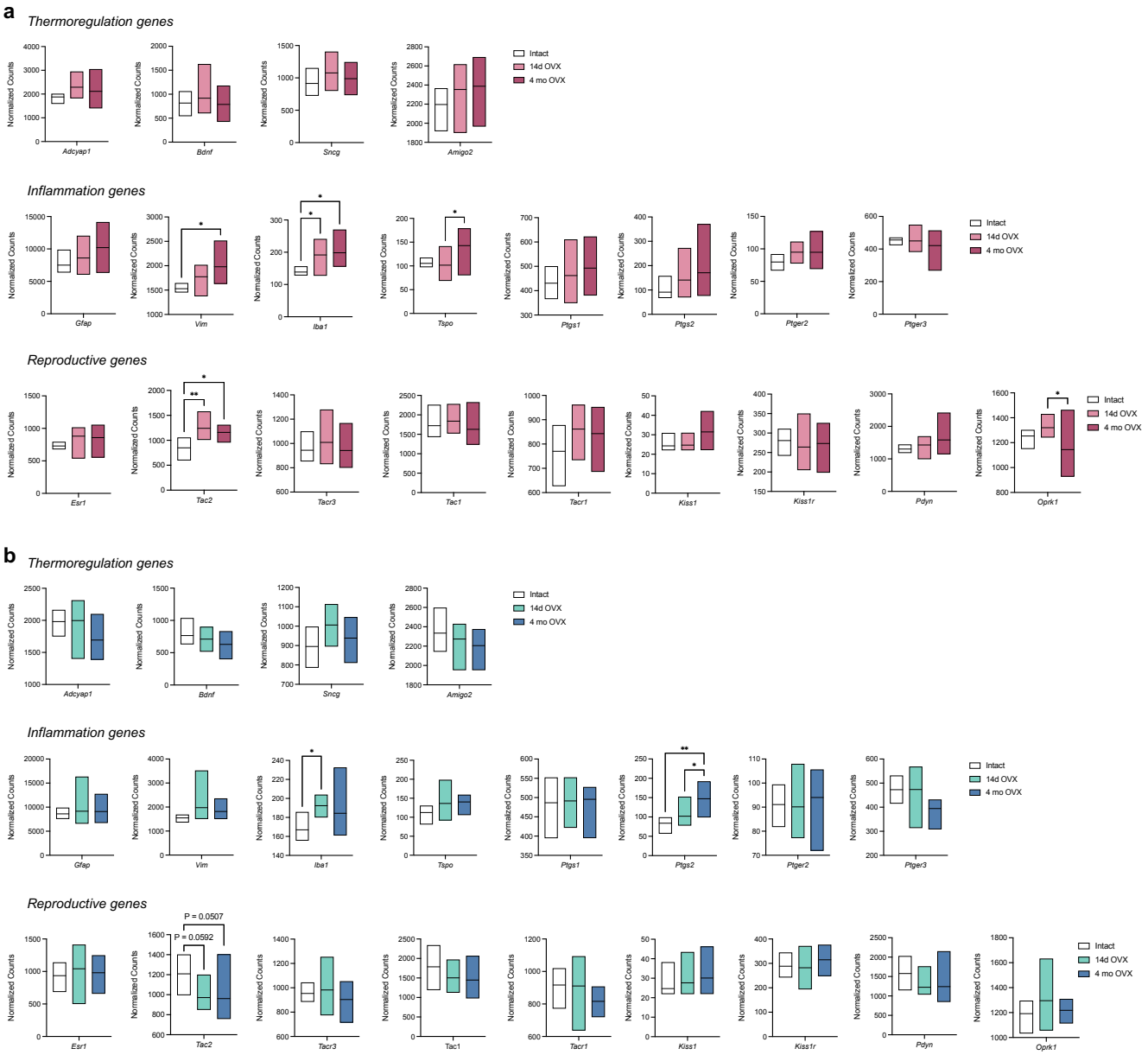

Figure 4. Expression of reproduction-, thermoregulation- and inflammation-related genes in short- and long-term post-ovariectomy mouse models.

a) Expression of KNDy genes and their receptors, thermoregulatory genes, astrocyte, and microglia marker genes between groups in the posterior hypothalamus (PH).

b) Expression of KNDy genes and their receptors, thermoregulatory genes, astrocyte, and microglia marker genes between groups in the preoptic area (POA).

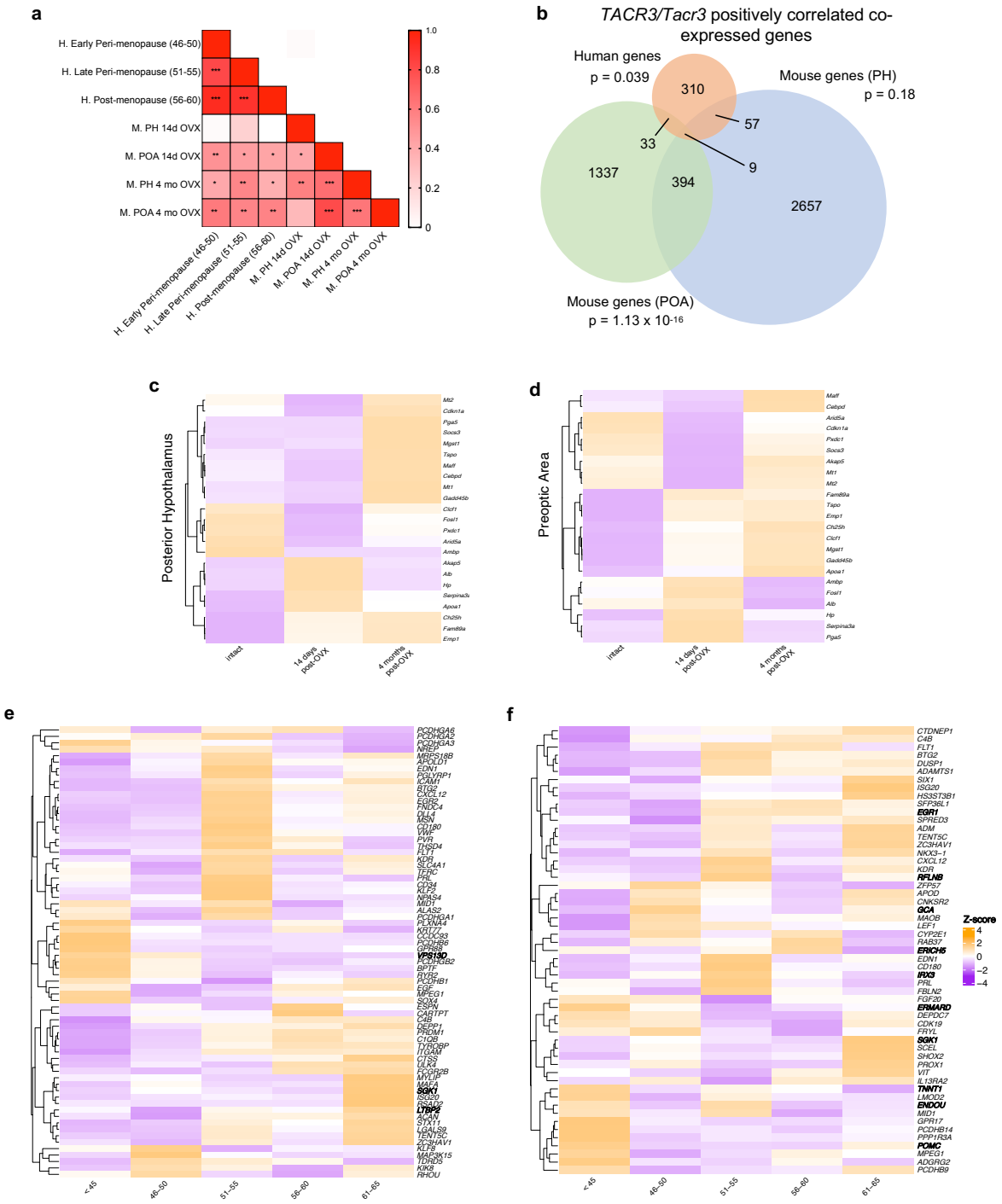

Figure 5. Comparative analysis of human and mouse hypothalamic reproductive aging datasets.

a) Heatmap of GSEA pathway correlations between human and mouse datasets; *p*-value from Pearson's correlation.

b) Overlap of *TACR3/Tacr3* positively correlated co-expressed genes between human and mouse; *p*-value from hypergeometric test.

Heatmap of identified DE genes from the human dataset and their expression across conditions in the mouse **c)** PH and **d)** POA datasets.
e) Heatmap of identified DE genes from the mouse PH and their expression across age groups in the human dataset.
f) Heatmap of identified DE genes from the mouse POA and their expression across age groups in the human dataset.

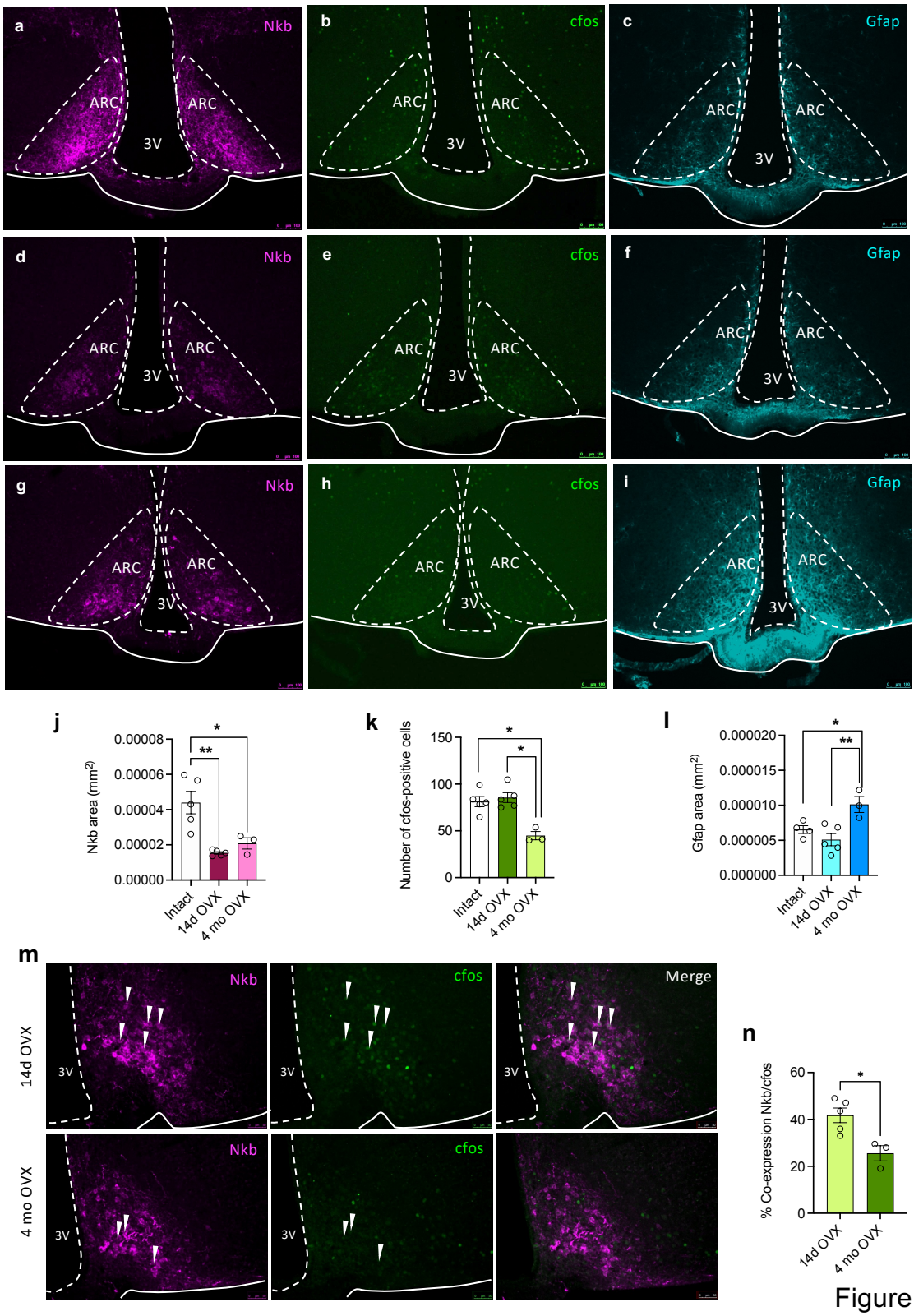

Figure 6

Figure 6. Differential neurokinin B distribution, neuronal activity and astrocyte reactivity within the arcuate nucleus from the short- and long-term post-ovariectomy mouse models.

783 Representative immunofluorescence staining of NKB, cFos and Gfap in the arcuate nucleus
784 (ARC) from intact **(a-c)**, 14 days post-OVX **(d-f)**, and 4 months post-OVX female mice **(g-i)**.
785 Quantification of NKB **(j)**, cFos **(k)**, and Gfap **(l)** in the ARC from intact, 14 days post- and 4
786 months post-OVX female mice.
787 m) Co-localization of NKB and cFos in the ARC from 14 days post- and 4 months post-OVX
788 female mice. Data from **j-l** and **n** shown as mean ± SEM. Statistical significance was
789 determinate by t-student Mann-Whitney test (intact vs. OVX).